MOLECULAR AND CELLULAR BIOLOGY, July 2004, p. 6467–6475 Vol. 24, No. 14
0270-7306/04/$08.00+0 DOI: 10.1128/MCB.24.14.6467–6475.2004

The E4F Protein Is Required for Mitotic Progression during Embryonic Cell Cycles

Laurent Le Cam,[1]† Matthieu Lacroix,[2] Maria A. Ciemerych,[1]‡ Claude Sardet,[2] and Piotr Sicinski[1]*

Department of Cancer Biology, Dana-Farber Cancer Institute, and Department of Pathology, Harvard Medical School, Boston, Massachusetts 02115,[1] and Institut de Génétique Moléculaire de Montpellier, CNRS UMR 5535, IFR122, 34293 Montpellier, France[2]

Received 15 January 2004/Returned for modification 29 February 2004/Accepted 9 April 2004

The ubiquitously expressed E4F protein was originally identified as an E1A-regulated cellular transcription factor required for adenovirus replication. The function of this protein in normal cell physiology remains largely unknown. To address this issue, we generated E4F knockout mice by gene targeting. Embryos lacking E4F die at the peri-implantation stage, while in vitro-cultured E4F$^{-/-}$ blastocysts exhibit defects in mitotic progression, chromosomal missegregation, and increased apoptosis. Consistent with these observations, we found that E4F localizes to the mitotic spindle during the M phase of early embryos. Our results establish a crucial role for E4F during early embryonic cell cycles and reveal an unexpected function for E4F in mitosis.

The products of the adenovirus early region 1A (*E1A*) gene are potent oncoproteins. E1A was shown to subvert cell proliferation in part by targeting essential cell cycle regulators such as the retinoblastoma tumor suppressor protein. This, in turn, leads to the release of the cellular transcription factors of the E2F family, which then stimulate transcription of the adenoviral *E2* gene and of cellular genes that are critical for the $G_1 \rightarrow S$-phase progression (21, 30, 35). In addition to the E2F transactivators, the E1A 13S oncoprotein regulates the activity of another cellular transcription factor, termed E4F, that was shown to be required for transcription of the adenoviral E4 gene (18, 20). Unlike the much-studied E2Fs, the cellular function of E4F is poorly understood. The E4F gene encodes a ubiquitously expressed 120-kDa protein, p120^{E4F}, that is structurally homologous to transcription factors of the GLI/Kruppel family. Upon E1A expression, p120^{E4F} is proteolytically cleaved, yielding a 50-kDa protein, p50^{E4F}, which is believed to represent a transcriptionally active form (7, 17, 18, 20). Although both p50^{E4F} and p120^{E4F} can recognize the same DNA sequence in vitro (7), they very likely differentially regulate gene expression in vivo. Thus, while p50^{E4F} is believed to act as a transcriptional activator, overexpression of p120^{E4F} was shown to repress transcription of the viral E4 and E1A genes (9) and of the cellular *cyclin A2* gene (4). This repressive action of p120^{E4F} might rely on E4F's direct interaction with histone deacetylase 1 (2).

Unlike the well-described cellular roles of other E1A targets, the physiological function of E4F remains largely unknown. It has been reported that ectopic expression of p120^{E4F} inhibits $G_1 \rightarrow S$-phase progression in various in vitro-cultured cell lines (8). Importantly, this E4F-mediated cell cycle arrest is reduced in pRB- or p53-deficient cells (5, 27), suggesting a genetic interaction between E4F and these two tumor suppressor pathways. Consistent with this notion, E4F was found to physically interact with pRB (5) and p53 (27). Other reports indicated that the ability of p120^{E4F} to block cell cycle progression might involve its physical interaction with p14^{ARF} (22), an increased expression of the p21^{Cip1} and p27^{Kip1} cell cycle inhibitors (8), or transcriptional repression of the *cyclin A2* gene (4).

To probe the physiological functions of the E4F protein, we inactivated the murine *E4F* locus by gene targeting in embryonic stem (ES) cells, and we generated E4F-null embryos. Our analyses revealed that E4F knockout (KO) embryos die at the peri-implantation stage and show mitotic progression defects, chromosomal missegregation and increased apoptosis. We found that these mitotic abnormalities correlate with E4F's association with the mitotic apparatus. Our results establish an unexpected function for E4F in mitosis during early embryonic cell cycles.

MATERIALS AND METHODS

E4F gene targeting vector. Several overlapping genomic fragments encompassing the mouse *E4F* gene were isolated by screening a lambda phage (provided by A. McClatchey, Massachusetts General Hospital, Boston, Mass.) and a bacterial artificial chromosome (Research Genetics) genomic library derived from the mouse strain 129SvJ, with the full-length human *E4F* cDNA as a probe. Exons 3 to 14 of the mouse E4F gene were replaced with a phosphoglycerokinase (PGK)-puromycin poly(A) resistance cassette placed in the orientation opposite to that of *E4F* transcription. In addition to the resistance cassette, additional EcoRI and NarI sites were introduced for screening purposes. The genomic fragments used for homologous recombination were composed of a 3.8-kb XhoI-KpnI fragment including part of the E4F promoter region, exons 1 and 2 for the 5′ arm, and a 4.5-kb Avr II fragment located downstream of exon 14 of the *E4F* gene for the 3′ arm. Our targeting vector also included a PGK-thymidine kinase-poly(A) cassette to allow for enrichment of targeted ES cells with ganciclovir. The E4F targeting vector was linearized with NotI and introduced into ES cells by electroporation with a Gene Pulser (1 pulse of 0.4 kV and 25 μF; Bio-Rad). The cells were subsequently cultured for 3 days in the presence of puromycin (2 μg/ml) and ganciclovir (2 μM) and then maintained only in puromycin for six additional days. Resistant ES cell clones were maintained on a monolayer of triple resistant (neomycin, puromycin, and hygromycin) feeders and cultured in conditioned ES

* Corresponding author. Mailing address: Dana-Farber Cancer Institute, 44 Binney St., Boston, MA 02115. Phone: (617) 632-5005. Fax: (617) 632-5006. E-mail: peter_sicinski@dfci.harvard.edu.

† Present address: Institut de Génétique Moléculaire de Montpellier, CNRS UMR 5535, IFR122, Montpellier, France.

‡ Present address: Department of Embryology, Institute of Zoology, Warsaw University, 02-096 Warsaw, Poland.

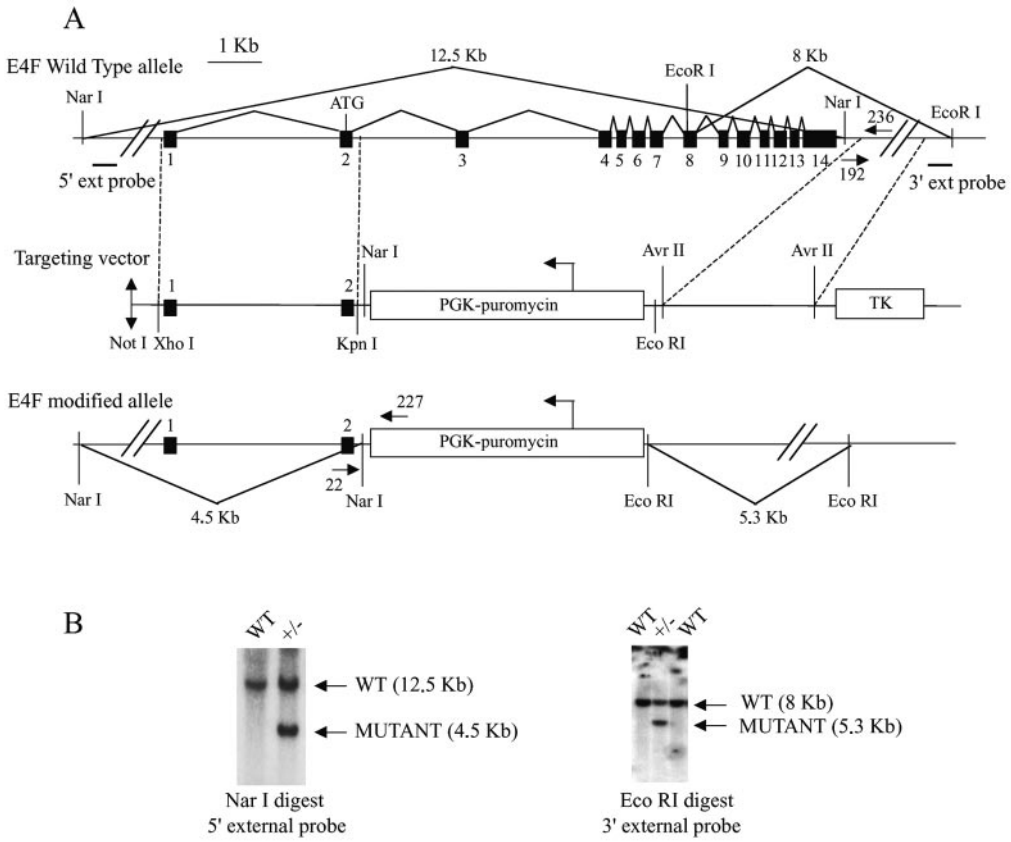

FIG. 1. Targeting strategy of the E4F locus. (A) Structure of the mouse E4F locus, the targeting vector, and the targeted allele after the homologous recombination. Solid boxes denote exons. Only restriction sites relevant to the targeting construct and to the screening strategies are indicated. (B) Southern blot analysis of a representative E4F$^{+/-}$ ES cell clone. Genotypes are shown above each lane. Homologous recombination on both ends was verified using external digests and external probes. For each digestion (NarI or EcoRI), the bands representing the WT and mutant alleles are indicated. The genomic fragments used as probes are shown in panel A. PGK, phosphoglycerokinase promoter; TK, thymidine kinase.

medium composed of ES Dulbecco's modified Eagle's medium (KO DMEM; GIBCO BRL) supplemented with leukemia inhibitory factor (550 ng/ml; Chemicon), 15% heat-inactivated fetal bovine serum (HyClone), 2 mM L-glutamine (GIBCO), 0.1 mM nonessential amino acid solution (GIBCO BRL), penicillin G (100 U/ml), streptomycin sulfate (100 μg/ml), and 50 μM β-mercaptoethanol. Homologous recombination was verified by Southern blotting of genomic DNA prepared from puromycin-resistant ES cell clones, by using external digests and external probes as indicated in Fig. 1B. Several correctly targeted E4F$^{+/-}$ ES cell clones that were confirmed to carry a single copy integration at the *E4F* locus and displayed a normal karyotype were subsequently injected into C57BL/6 blastocysts and gave rise to germ line-transmitting chimeric mice.

Blastocyst culture and genotyping of preimplantation embryos. All embryos were generated by natural mating of E4F heterozygote animals. The morning of the day on which a vaginal plug was detected was designated as day E0.5. Embryos were collected on E3.5 or E4.5 by flushing the uteri with M2 medium (Sigma). Embryos were then either fixed immediately or cultured in ES complete medium for the appropriate time.

For genotyping, individual embryos were lysed by incubation at 55°C overnight in 5 μl (for the blastocysts) or 100 μl (for E9.5 embryos) of PCR lysis buffer (10 mM Tris-HCl, pH 8.0, 50 mM KCl, 2 mM $MgCl_2$, 0.45% NP-40, 0.45% Tween 20, 0.2 mg of proteinase K/ml). To detect the wild-type (WT) and mutant E4F alleles, PCRs were performed with the following primers: E4F WT allele, primer #192 (5′ AGGTCTGCTAGGGTATGAGG) and primer #236 (5′ GCCCTAG CCTGCTCTGCCATC); E4F mutant allele, primer #22 (5′ CACTGCCTTGG AGGACTTTG) and primer #227 (5′ CCTCTGTTCCACATACACTTCAT TC). The amplification protocol included an initial incubation step at 94°C for 5 min, followed by 35 cycles with each cycle comprised of 1-min denaturation at 94°C, 1-min annealing at 55°C, and 1 min of elongation at 72°C, with AmpliTaq Gold polymerase (Applied Biosystems).

Immunocytochemistry and terminal deoxynucleotidyltransferase-mediated dUTP-biotin nick end labeling (TUNEL) staining. Embryos were washed two times in phosphate-buffered saline (PBS), fixed in 4% paraformaldehyde in PBS for 30 min at 4°C, and then permeabilized for 20 min at room temperature in PBS containing 0.3% Triton X-100 and 1.5% bovine serum albumin. For BrdU-treated embryos, DNA was denatured after the permeabilization step with 2 N HCl–0.5% Triton X-100 for 20 min at room temperature and then washed extensively in PBS with 1.5% bovine serum albumin. Embryos were incubated under mineral oil with specific primary antibodies overnight at 4°C. The anti-Bub1 (clone 4B12) and anti-BubR1/Mad3 (clone 5F9) monoclonal antibodies and the polyclonal anti-CENP-E antibody were kindly provided by F. McKeon (Harvard Medical School, Boston, Mass.) and by D. Cleveland (University of California, San Diego). The polyclonal anti-phospho-(ser10) histone H3 antibody was from Upstate Biotechnology, the anti-α-tubulin (clone T9026) was from Sigma, and the monoclonal anti-BrdU antibody was from Becton Dickinson. The affinity-purified anti-E4F polyclonal antibody was raised against residues 358 to 784 of the human E4F protein (5). Cy-3 or fluorescein isothiocyanate-conjugated secondary antibodies (Jackson Immunoresearch Laboratory) and DAPI (4′,6′-diamidino-2-phenylindole) were incubated for 4 h at room temperature. DNA fragmentation associated with apoptosis was detected with an in situ cell death detection kit (Roche).

RESULTS

Generation of E4F-deficient mice. We cloned the mouse *E4F* gene and determined its exon-intron structure. The human and murine *E4F* genes, located on chromosomes 16p13.3 and 17, respectively (24, 26), share a highly conserved genomic organization composed of 14 exons spread over the distance of

TABLE 1. Genotypes of progeny from E4F heterozygous mating[a]

Age (dpc)	No. per genotype			No. (%) resorbed	Total
	+/+	+/−	−/−		
Adult	122	244	0	NA	366
13.5	12	17	0	11 (27)	40
11.5	8	19	0	9 (25)	36
9.5	19	17	0	14 (28)	50
7.5	10	25	0	12 (26)	47
5.5	3	13	4	2 (9)	22
3.5	81	164	68	NA	313

[a] NA, not applicable; dpc, days postcoitum.

approximately 12 kb (Fig. 1A). In our gene targeting strategy, we replaced exons 3 to 14 of the murine *E4F* gene (which together encode amino acids 104 to 784 of the E4F protein) by a puromycin resistance cassette (Fig. 1A). This large deletion removes all C2H2 zinc-finger domains which are responsible for E4F DNA binding and functional activities (5, 8, 25).

The E4F targeting construct was electroporated into J1 embryonic stem (ES) cells, and puromycin-resistant clones were screened for homologous recombination by Southern blotting, as indicated in Fig. 1B. $E4F^{+/-}$ ES cells were injected into C57BL/6 blastocysts and gave rise to germ line-transmitting chimeric mice. These mice were backcrossed to C57BL/6 animals, yielding E4F heterozygotes. The results reported below were obtained with two independently derived E4F-deficient strains.

E4F is essential for early embryogenesis. Heterozygous $E4F^{+/-}$ mice were phenotypically normal, healthy, and fertile with no developmental or histological abnormalities detectable over a 20-month observation period (data not shown). In contrast, no homozygous E4F-null animals were detected among 366 live births from $E4F^{+/-}$ intercrosses (Table 1), indicating that one functional E4F allele is sufficient to support full embryonic and adult tissue development, whereas inactivation of both alleles leads to embryonic lethality.

To assess the time of E4F KO developmental failure, embryos from heterozygote intercrosses were collected at different times of gestation and genotyped by PCR. No homozygous mutant embryos were recovered at E7.5 or beyond (Table 1). However, we observed empty deciduae at an approximately 1 in 4 ratio, suggesting that E4F-deficient embryos died after the implantation (Table 1). To verify this notion, the entire uteri containing E5.5 embryos were processed for histological analyses. Embryos were laser captured from the sections and were genotyped by PCR. We found that $E4F^{-/-}$ embryos were either completely resorbed or markedly abnormal. In the latter case, mutant embryos exhibited greatly reduced size and displayed no detectable layer organization (Fig. 2A, lower panels).

We also collected embryos at day E4.5 by flushing the uteri of pregnant females, and we analyzed their appearance. We found that E4F-deficient E4.5 embryos were severely growth retarded compared to control littermates (Fig. 2A, upper right panel). In contrast, mutant blastocyst stage embryos flushed out at E3.5 ($n = 68$) were virtually indistinguishable from WT ($n = 164$) or heterozygous ($n = 81$) littermates (Fig. 2A, upper left panel). Visualization of cell nuclei by DAPI staining revealed that all E3.5 blastocysts were composed of 53 ± 8 cells,

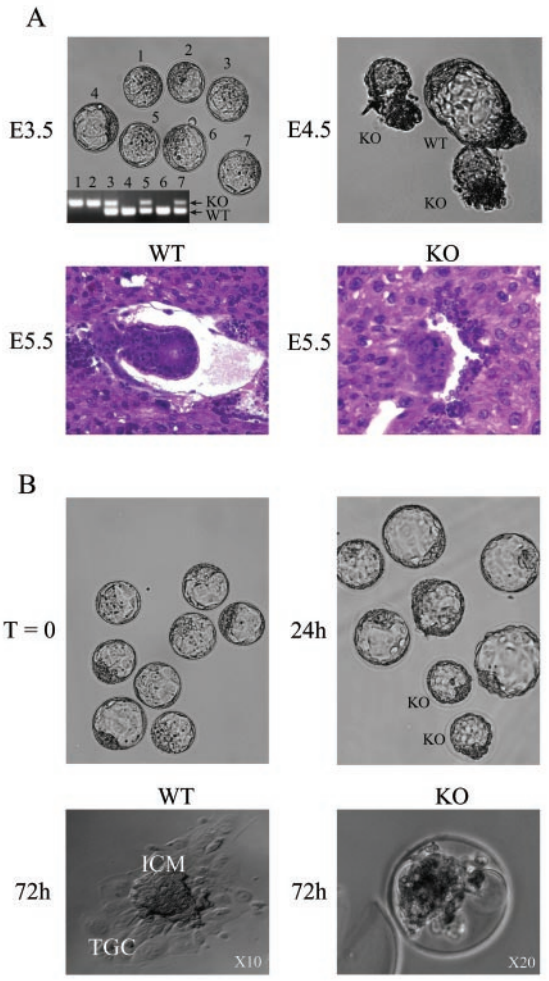

FIG. 2. E4F disruption results in early embryonic lethality. (A) The appearance of mutant embryos. Upper panels, E3.5 and E4.5 embryos were flushed out from the uteri and were photographed under bright field conditions. E3.5 blastocysts were subsequently genotyped by PCR. Note normal appearance of mutant embryos at E3.5 and severe growth retardation at E4.5. Lower panels, the appearance of E5.5 embryos developing in utero, as revealed by hematoxylin and eosin staining of histologic sections. A typical picture of a WT and of a not yet fully resorbed $E4F^{-/-}$ embryo is shown. (B) Impaired in vitro development of E4F-deficient embryos. Blastocyst stage embryos were flushed from the uterus at E3.5, cultured in vitro for several days, and subsequently genotyped by PCR. While all the littermates displayed similar morphology at E3.5 (upper left panel), $E4F^{-/-}$ embryos appeared growth retarded after 24 h of culture (upper right panel). After 72 h of in vitro culture, WT and $E4F^{+/-}$ embryos developed outgrowths composed of the inner cell mass (ICM) surrounded by a single layer of trophoblast giant cells (TGC) (lower left panel), whereas $E4F^{-/-}$ embryos degenerated inside the zonae pellucidae (lower right panel).

irrespective of their genotype ($n = 10$ for each genotype). Collectively, these observations revealed that E4F-deficient embryos fail at the peri-implantation stage.

To further characterize the developmental abnormalities of E4F-deficient embryos, we isolated E3.5 blastocysts derived from $E4F^{+/-} \times E4F^{+/-}$ crosses and cultured them in vitro for several days. As expected, WT or heterozygous embryos expanded after 24 h of culture and later hatched from their zonae

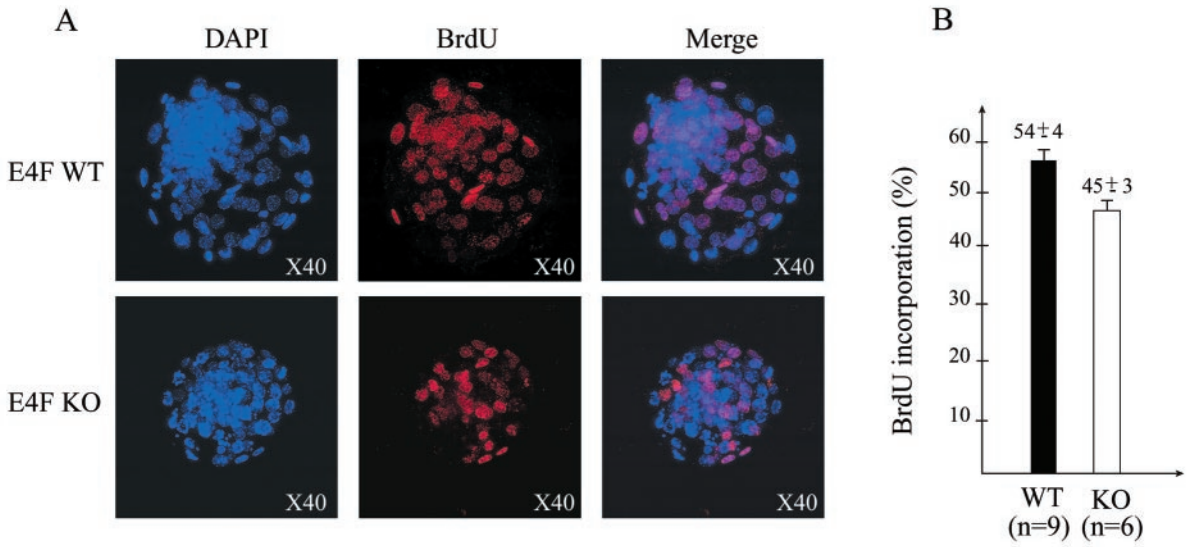

FIG. 3. S-phase progression in E4F-deficient embryos. (A) S-phase progression was gauged by determining BrdU incorporation in blastocysts recovered from $E4F^{+/-}$ intercrosses. Embryos were cultured in vitro for 24 h, pulsed for 20 min with BrdU, and processed for BrdU immunostaining and DAPI counterstaining. (B) Series of Z-plane images were stacked and analyzed by deconvolution microscopy to precisely quantify the percentage of BrdU-positive cells in WT and $E4F^{-/-}$ blastocysts after 24 h of culture. Error bars indicate standard deviations.

pellucidae to form a prominent inner cell mass outgrowth on a flat patch of trophectoderm cells. In contrast, none of the $E4F^{-/-}$ embryos hatched, and they degenerated inside the zonae pellucidae after 3 days of in vitro culture (Fig. 2B). The difference between WT (and $E4F^{+/-}$) versus $E4F^{-/-}$ embryos was already obvious after 24 h of in vitro culture (i.e., at a stage roughly corresponding to E4.5). At this time point, $E4F^{-/-}$ embryos were invariably smaller than heterozygous or WT littermates (Fig. 2B, upper right panel) and were composed of only 88 ± 10 cells ($n = 9$), compared with 126 ± 13 cells ($n = 9$) in WT embryos. Hence, our in vivo and in vitro analyses indicate that the E4F gene is critically required during early embryogenesis.

Cell cycle progression of $E4F^{-/-}$ embryonic cells. We next used the in vitro blastocyst cultures to ascertain whether the developmental failure of E4F-deficient embryos was the consequence of cell proliferation defects. In the initial set of experiments, E3.5 blastocysts that had been cultured in vitro for 24 h were pulse-labeled for 20 min with 5-bromo-2-deoxyuridine (BrdU), and BrdU-positive cells were quantitated by indirect immunofluorescence. As shown in Fig. 3, we detected on average 45% ± 3% of BrdU-positive cells in $E4F^{-/-}$ embryos ($n = 6$), compared to 54% ± 4% in control littermates ($n = 9$). Although statistically significant (Mann-Whitney test, $P = 0.05$), this small difference cannot fully explain the 30% decrease in cell number observed in E4F-deficient blastocysts after 24 h of in vitro culture, given that the cell division doubling time at that developmental stage is close to 20 h (10). These data suggested to us the existence of additional abnormalities in E4F-deficient embryos.

Mitotic progression defects in E4F-deficient embryos. We next turned our attention to the M-phase progression in E4F-deficient cells. To this end, we immunostained WT and $E4F^{-/-}$ blastocysts with an antibody against histone H3 phosphorylated on serine 10 (HH3 P-Ser10), a common mitotic marker used to mark M-phase cells (11). We found that all freshly isolated E3.5 blastocysts showed a very similar proportion of phosphohistone H3-positive (i.e., mitotic) cells, irrespective of their genotype (approximately 3% of cells; Fig. 4B). In contrast, after 24 h of in vitro culture, the mitotic index of E4F-deficient embryos was threefold higher than that of WT littermates (Fig. 4A and B).

Careful examination of mitotic figures in $E4F^{-/-}$ embryos revealed that an unusually large proportion of them corresponded to the prometaphase stage, a phase during which chromosomes are already fully condensed but not yet aligned on the metaphase plate (68% of all mitotic figures analyzed in E4F-deficient, $n = 88$, versus 32% in WT embryos, $n = 66$; Fig. 4C and D). Consequently, metaphase, anaphase, and telophase mitotic figures were observed less frequently in E4F-deficient embryos than in the WT counterparts (Fig. 4D), suggesting a mitotic progression failure in the absence of E4F.

To further ascertain whether the observed accumulation of cells in mitosis was indeed the result of a mitotic arrest, we examined the ability of E4F-deficient cells to exit mitosis. To this end, we cultured embryos in vitro for 24 h (a time point when E4F KO embryos exhibit a fully penetrant phenotype) and then subjected them to 10 Gy of gamma irradiation, in order to activate their DNA damage checkpoint. In embryonic cells, this checkpoint does not trigger a mitotic arrest (16) but mainly induces a G_2 block (12, 15, 28, 31). Therefore, cells that are in the M phase at the time of irradiation are expected to exit mitosis, progress through the cell cycle, and finally accumulate at the next G_2 phase. As expected, upon gamma irradiation of WT embryos, we observed a strong decrease of the number of HH3 P-Ser 10-positive cells, revealing exit of cells from the M phase. In contrast, the proportion of mitotic cells remained unchanged in E4F-deficient embryos after the irradiation (Mann-Whitney test, $P = 0.05$) (Fig. 4E). These results suggest that in $E4F^{-/-}$ conceptuses, these HH3 P-Ser 10-pos-

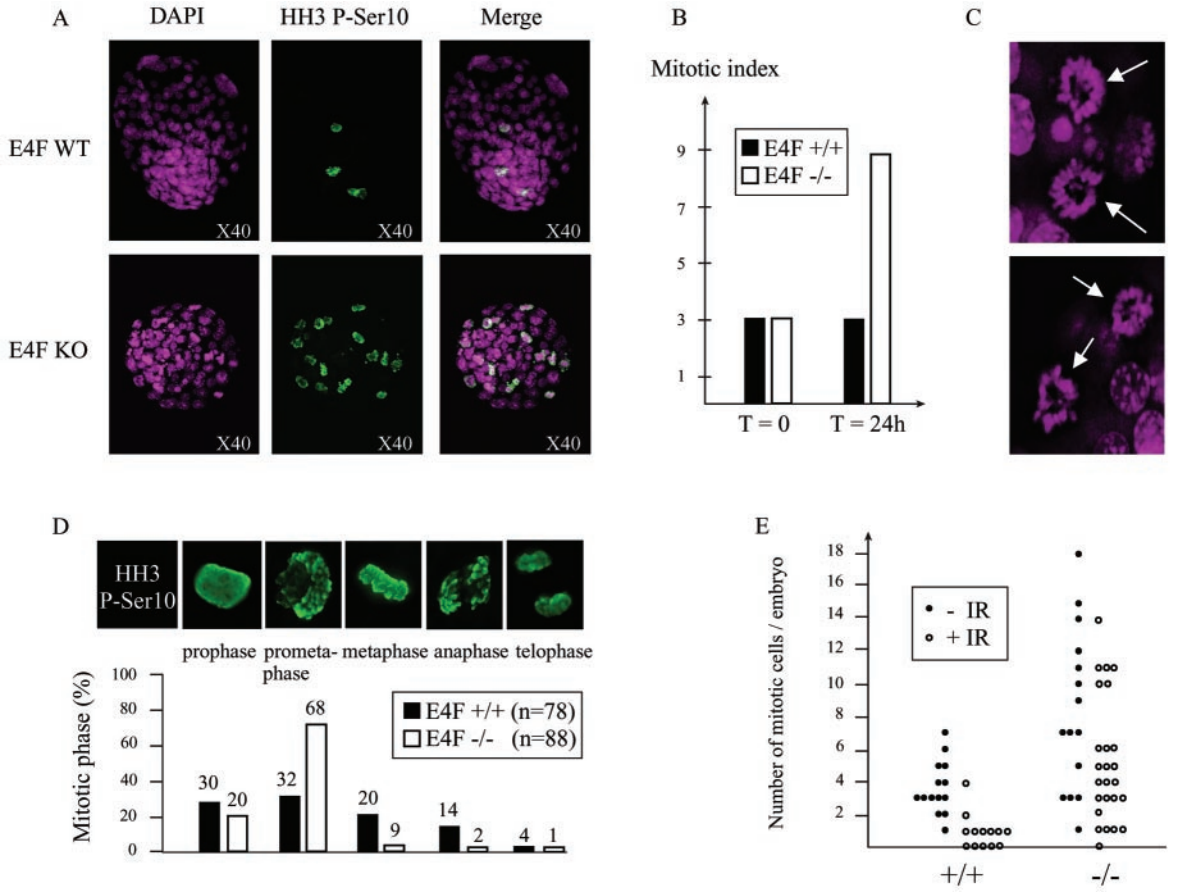

FIG. 4. M-phase progression defects in E4F-deficient embryos. (A) Increased mitotic index in E4F$^{-/-}$ embryos. Shown are representative WT and mutant littermates that were cultured in vitro for 24 h and then fixed and stained with antibody against phospho-(Ser 10) histone H3 (HH3 P-Ser10), a marker of mitotic cells. Nuclei were counterstained with DAPI. (B) The mitotic index in freshly isolated E3.5 embryos (T = 0) or in embryos cultured in vitro for 24 h (T = 24) was calculated as the mean number of HH3 P-Ser10-positive cells per embryo divided by the mean number of cells per embryo, times 100% (n = 15 for each genotype). (C and D) E4F$^{-/-}$ cells are blocked at the prometaphase stage. (C) Typical prometaphase figures (arrows) observed after DAPI staining of cultured E4F-deficient embryos. (D) Mitotic figures were identified in cultured WT and E4F$^{-/-}$ embryos based on the HH3 P-Ser10 immunostaining and were classified into the appropriate mitotic stage. The data are presented as percentages of these various stages among all M-phase cells. (E) Defective mitotic exit in E4F$^{-/-}$ embryos. Embryos were isolated at E3.5, cultured for 24 h, gamma irradiated, and left in culture for six additional hours. Embryos were then fixed, processed for the HH3 P-Ser10 immunostaining, and subsequently lysed individually for genotyping by PCR analysis. The number of mitotic cells (HH3 P-Ser10 positive) in nonirradiated (black circles) or irradiated embryos (open circles) is plotted according to their genotype.

itive cells are unable to exit mitosis but are instead arrested or "trapped" at the prometaphase stage. Altogether, our data suggest that E4F is critically required for M-phase progression in embryonic cells.

We next tried to address the molecular basis of the mitotic arrest seen in E4F-deficient embryos. We hypothesized that E4F$^{-/-}$ cells were blocked at the prometaphase stage due to the constitutive activation of their spindle checkpoint. The core components of this checkpoint were first identified in yeast and are highly conserved in mammals. These proteins, which include the protein kinases Bub1, BubR1 (also called Mad3), and the motor protein CENP-E (for a review, see reference 1), can be detected by immunofluorescence in mitotic cells with an activated spindle checkpoint (33).

In order to assess whether E4F$^{-/-}$ cells have activated their spindle checkpoint, we stained in vitro-cultured E4F-deficient blastocysts with antibodies against Bub1, BubR1, and CENP-E. Indeed, we observed that the kinetochores of E4F$^{-/-}$ mitotic cells were strongly labeled by anti-Bub1 (Fig. 5A), anti-BubR1 (Fig. 5B), and anti-CENP-E (data not shown) antibodies, indicating that E4F$^{-/-}$ cells are arrested in prometaphase with an activated spindle checkpoint.

When we analyzed the cellular localization of E4F in the early embryos by indirect immunofluorescence, we detected endogenous E4F protein in the nucleus of interphasic cells (data not shown), a localization consistent with the previously described function of E4F as a transcription factor. Notably, in mitotic cells, we noticed immunolabeling of E4F on the mitotic spindle which colocalized with α-tubulin (Fig. 6). In contrast, no staining of E4F was observed on the condensed mitotic chromosomes. Importantly, both interphasic and mitotic staining patterns were strongly reduced in E4F$^{-/-}$ blastocysts. In addition, preincubation of the anti-E4F antibody with recombinant full-length E4F protein completely abolished the staining in WT embryos (data not shown), demonstrating that this immunoreactivity is specific.

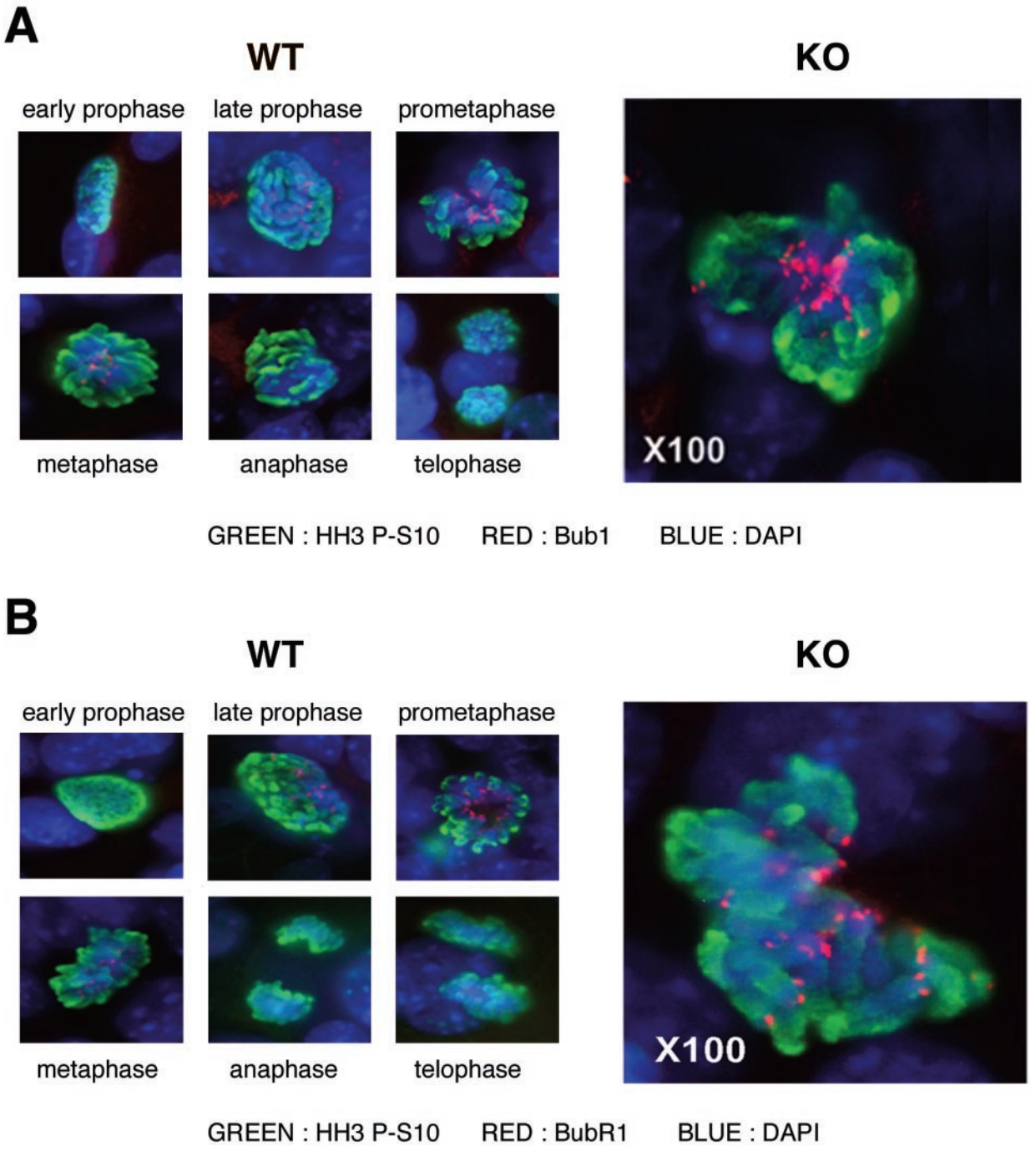

FIG. 5. Embryonic cells that lack E4F are arrested in prometaphase with an active spindle checkpoint, as revealed by Bub1 and BubR1 immunostaining. Examples of WT embryos, representing various phases of the M-phase progression, and representative E4F-deficient embryos (KO) were costained in panel A with anti-HH3 P-Ser10 antibodies, anti-Bub1 antibodies, and DAPI, or in panel B, with anti-HH3 P-Ser10 antibodies, anti-BubR1 antibodies, and DAPI.

Strikingly, we frequently noticed abnormal mitotic figures in E4F-deficient embryos, where one or two misaligned chromosomes were positioned far outside of the metaphase plate (Fig. 7A). In a total of more than 100 mitotic figures analyzed, 18% displayed abnormalities with misaligned chromosomes. Such abnormal mitotic figures were extremely rarely observed in normal embryos (1 in 100 analyzed).

Altogether, our data suggest that the lack of E4F results in the chronic activation of the spindle checkpoint and the arrest of E4F-deficient mitotic cells at the prometaphase stage and leads to chromosomal misalignment.

Increased cell death in E4F$^{-/-}$ embryos. We further hypothesized that the chromosomal segregation defects seen in E4F KO cells might eventually result in increased cell death in

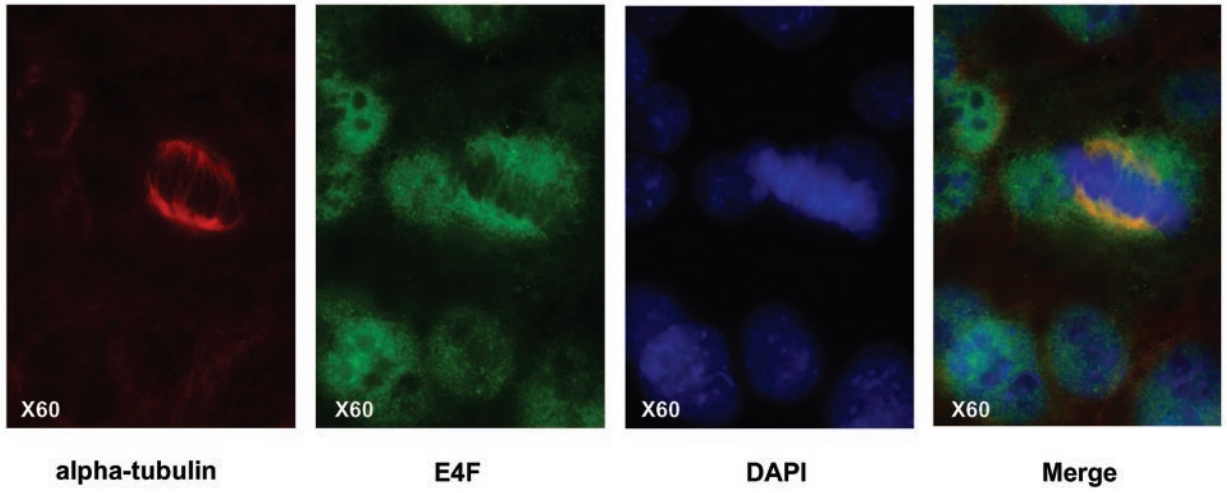

FIG. 6. E4F is localized on the mitotic spindle. WT blastocysts were immunostained with a specific anti-E4F antibody. The mitotic spindle was visualized by α-tubulin immunostaining. Nuclei were counterstained with DAPI.

mutant conceptuses, leading to the death of the entire embryo. Consistent with this hypothesis, DAPI staining revealed the presence of numerous condensed and fragmented nuclei, a hallmark of apoptotic cells, in in vitro-cultured E4F-deficient embryos. We further confirmed this observation by TUNEL staining. Our analyses revealed that apoptotic cells were rarely detected in freshly isolated E3.5 blastocysts, irrespective of the embryo genotype (data not shown). However, after 24 h of in vitro culture, TUNEL-positive cells were readily detected in $E4F^{-/-}$ embryos but were rarely observed in their heterozygous or WT littermates (Fig. 7B). Collectively, these results suggest that cell death is responsible, at least in part, for the demise of E4F-deficient embryos.

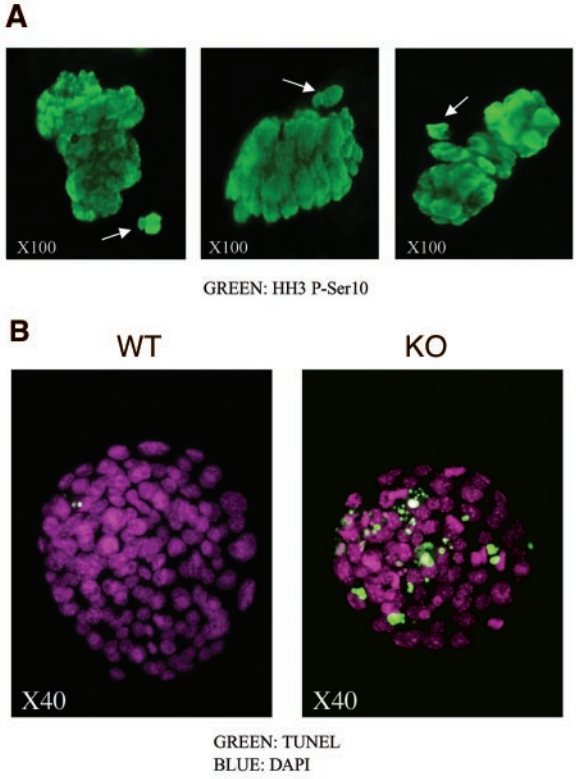

FIG. 7. $E4F^{-/-}$ embryos exhibit abnormal mitotic figures and increased cell death. (A) Mitotic cells in in vitro-cultured blastocysts were identified by HH3 P-Ser10 immunostaining. Examples of abnormal mitotic figures seen in E4F-deficient embryos are shown. Arrows indicate misaligned chromosomes. (B) Increased apoptosis in E4F-deficient embryos. Merged image obtained from representative WT and $E4F^{-/-}$ blastocysts cultured for 24 h and processed for DAPI and TUNEL staining.

DISCUSSION

In this study, we generated a mouse mutant for the *E4F* gene. The product of this gene was originally identified as a cellular protein activated by the viral E1A oncoprotein during adenoviral infection (13, 18, 20). Our analyses of E4F-deficient embryos demonstrated a critical and nonredundant function for E4F during early murine embryogenesis between days E3.5 and E5.5. Normal development of $E4F^{-/-}$ embryos prior to day E3.5 might suggest that E4F is dispensable at these very early embryonic stages. Alternatively, we reason that the normal development of E4F-deficient embryos up to the blastocyst stage may rely on protein stocks of maternal origin.

By using an in vitro outgrowth model that recapitulated the in vivo developmental failure of E4F-deficient embryos, we showed that $E4F^{-/-}$ conceptuses exhibit mitotic progression defects. Our analyses revealed that E4F-deficient cells are blocked at the prometaphase stage with an activated spindle checkpoint. It is interesting that several mouse strains engineered to lack proteins involved in the spindle checkpoint also die at the peri-implantation stage, with mitotic abnormalities resembling the ones found in E4F-deficient embryos. These strains include the *Mad2* (32), the *survivin* (34), the *Incenp* (3), and *CENP-E* mutant mice (19). However, our results clearly indicate that in contrast to the Mad2- and CENP-E-null embryos, E4F-deficient blastocysts display an increased mitotic index, supporting the idea that $E4F^{-/-}$ embryos have a functional spindle checkpoint. One possibility is that—in a manner similar to survivin-depleted cells (14)—$E4F^{-/-}$ cells cannot

permanently sustain this mitotic arrest, and they finally exit mitosis in an aberrant manner. Consistent with this model, we frequently observed abnormal mitotic figures with misaligned chromosomes in E4F-deficient embryos.

While it is our prediction that the increased cell death seen in E4F-deficient embryos is the consequence of the mitotic and chromosomal abnormalities observed in E4F-null mutants, our data do not allow us to formally rule out an independent function for E4F in controlling apoptosis in embryonic cells.

Surprisingly, while E4F overexpression-based experiments suggested an important role for this transcription factor at the G_1/S transition, we have not detected any major abnormalities in the ability of E4F KO embryos to incorporate BrdU. However, we found that the knockdown of the E4F mRNA by RNA interference in in vitro-cultured NIH 3T3 fibroblasts resulted in a strong inhibition of BrdU incorporation (data not shown). These results suggest that E4F may have different functions in early embryonal cells versus those in cells at later stages of development. Interestingly, a recent report revealed that overexpression of $p120^{E4F}$ in fibroblasts led to the formation of a subset of tetraploid and multinucleated cells (23), raising a possibility that E4F may also play roles in mitosis in these cells. The availability of an E4F conditional KO strain should greatly facilitate analyses of E4F's function in various cell types.

We do not know at present whether the function of E4F in cell cycle progression of early embryonic cells involved E4F's transcriptional activities. In this regard, E4F target genes that may play a role in mitotic progression remain unknown. The work of Fajas et al. indicated that E4F acts as a transcriptional regulator of the *cyclin A2* gene (4). However, this target gene is likely not involved in the observed embryonic defect since our analyses (data not shown), as well as that of other laboratories (36), demonstrated that cyclin A2 is not expressed in blastocysts. Based on the localization of the E4F protein to the mitotic spindle in M-phase cells, we propose that E4F plays a direct role in mitosis, possibly in chromosome congression. This function is likely independent from the role of E4F as a transcription factor. Consistent with this hypothesis, while this paper was under review, Fenton et al. reported that $p120^{E4F}$ physically interacts with the tumor suppressor gene product RASSF1A (6). RASSF1 was recently demonstrated to be involved in controlling mitotic progression through the inhibition of the ubiquitin ligase activity of the Cdc20–anaphase-promoting complex (29). Collectively, these findings point to an intriguing possibility that E4F may be also involved in the regulation of anaphase-promoting complex functions. Further experiments will be required to address this hypothesis.

ACKNOWLEDGMENTS

We thank Rod Bronson for help with histopathological analyses, F. McKeon and D. Cleveland for plasmids and reagents, J. Alberta and M. Donohoe for technical assistance, and A. Le Cam, T. Makela, L. Kim, and R. Hipskind for critical reading of the manuscript. We are grateful to all members of the Sicinski's laboratory for their support and technical help and to C. Bouchard for help with statistical analyses.

This work was funded by the Susan Komen Breast Cancer Foundation grant to P.S. L.L. was supported by postdoctoral fellowships from La Ligue contre le Cancer and the Human Frontier Science Program, M.L. by a predoctoral MNRT fellowship, and M.A.C. by International Agency for Research on Cancer and Kosciuszko Foundation fellowships. C.S. is funded by the French Ligue Nationale contre le Cancer (Equipe Labelisée 2003).

REFERENCES

1. **Cleveland, D. W., Y. Mao, and K. F. Sullivan.** 2003. Centromeres and kinetochores: from epigenetics to mitotic checkpoint signaling. Cell **112:**407–421.
2. **Colombo, R., G. F. Draetta, and S. Chiocca.** 2003. Modulation of p120E4F transcriptional activity by the Gam1 adenoviral early protein. Oncogene **22:**2541–2547.
3. **Cutts, S. M., K. J. Fowler, B. T. Kile, L. L. Hii, R. A. O'Dowd, D. F. Hudson, R. Saffery, P. Kalitsis, E. Earle, and K. H. Choo.** 1999. Defective chromosome segregation, microtubule bundling and nuclear bridging in inner centromere protein gene (Incenp)-disrupted mice. Hum. Mol. Genet. **8:**1145–1155.
4. **Fajas, L., C. Paul, A. Vie, S. Estrach, R. Medema, J. M. Blanchard, C. Sardet, and M. L. Vignais.** 2001. Cyclin A is a mediator of $p120^{E4F}$-dependent cell cycle arrest in G_1. Mol. Cell. Biol. **21:**2956–2966.
5. **Fajas, L., C. Paul, O. Zugasti, L. Le Cam, J. Polanowska, E. Fabbrizio, R. Medema, M. L. Vignais, and C. Sardet.** 2000. pRB binds to and modulates the transrepressing activity of the E1A-regulated transcription factor p120E4F. Proc. Natl. Acad. Sci. USA **97:**7738–7743.
6. **Fenton, S. L., A. Dallol, A. Agathanggelou, L. Hesson, J. Ahmed-Choudhury, S. Baksh, C. Sardet, R. Dammann, J. D. Minna, J. Downward, E. R. Maher, and F. Latif.** 2004. Identification of the E1A-regulated transcription factor p120 E4F as an interacting partner of the RASSF1A candidate tumor suppressor gene. Cancer Res. **64:**102–107.
7. **Fernandes, E. R., and R. J. Rooney.** 1997. The adenovirus E1A-regulated transcription factor E4F is generated from the human homolog of nuclear factor phiAP3. Mol. Cell. Biol. **17:**1890–1903.
8. **Fernandes, E. R., J. Y. Zhang, and R. J. Rooney.** 1998. Adenovirus E1A-regulated transcription factor $p120^{E4F}$ inhibits cell growth and induces the stabilization of the cdk inhibitor $p21^{WAF1}$. Mol. Cell. Biol. **18:**459–467.
9. **Fognani, C., G. Della Valle, and L. E. Babiss.** 1993. Repression of adenovirus E1A enhancer activity by a novel zinc finger-containing DNA-binding protein related to the GLI-Kruppel protein. EMBO J. **12:**4985–4992.
10. **Harlow, G. M., and P. Quinn.** 1982. Development of preimplantation mouse embryos in vivo and in vitro. Aust. J. Biol. Sci. **35:**187–193.
11. **Hendzel, M. J., Y. Wei, M. A. Mancini, A. Van Hooser, T. Ranalli, B. R. Brinkley, D. P. Bazett-Jones, and C. D. Allis.** 1997. Mitosis-specific phosphorylation of histone H3 initiates primarily within pericentromeric heterochromatin during G2 and spreads in an ordered fashion coincident with mitotic chromosome condensation. Chromosoma **106:**348–360.
12. **Hirao, A., Y. Y. Kong, S. Matsuoka, A. Wakeham, J. Ruland, H. Yoshida, D. Liu, S. J. Elledge, and T. W. Mak.** 2000. DNA damage-induced activation of p53 by the checkpoint kinase Chk2. Science **287:**1824–1827.
13. **Lee, K. A., and M. R. Green.** 1987. A cellular transcription factor E4F1 interacts with an E1a-inducible enhancer and mediates constitutive enhancer function in vitro. EMBO J. **6:**1345–1353.
14. **Lens, S. M., R. M. Wolthuis, R. Klompmaker, J. Kauw, R. Agami, T. Brummelkamp, G. Kops, and R. H. Medema.** 2003. Survivin is required for a sustained spindle checkpoint arrest in response to lack of tension. EMBO J. **22:**2934–2947.
15. **Liu, Q., S. Guntuku, X. S. Cui, S. Matsuoka, D. Cortez, K. Tamai, G. Luo, S. Carattini-Rivera, F. DeMayo, A. Bradley, L. A. Donehower, and S. J. Elledge.** 2000. Chk1 is an essential kinase that is regulated by Atr and required for the G(2)/M DNA damage checkpoint. Genes Dev. **14:**1448–1459.
16. **Mikhailov, A., R. W. Cole, and C. L. Rieder.** 2002. DNA damage during mitosis in human cells delays the metaphase/anaphase transition via the spindle-assembly checkpoint. Curr. Biol. **12:**1797–1806.
17. **Nevins, J. R.** 1990. Adenovirus E1A-dependent trans-activation of transcription. Semin. Cancer Biol. **1:**59–68.
18. **Nevins, J. R., P. Raychaudhuri, A. S. Yee, R. J. Rooney, I. Kovesdi, and R. Reichel.** 1988. Transactivation by the adenovirus E1A gene. Biochem. Cell Biol. **66:**578–583.
19. **Putkey, F. R., T. Cramer, M. K. Morphew, A. D. Silk, R. S. Johnson, J. R. McIntosh, and D. W. Cleveland.** 2002. Unstable kinetochore-microtubule capture and chromosomal instability following deletion of CENP-E. Dev. Cell **3:**351–365.
20. **Raychaudhuri, P., R. Rooney, and J. R. Nevins.** 1987. Identification of an E1A-inducible cellular factor that interacts with regulatory sequences within the adenovirus E4 promoter. EMBO J. **6:**4073–4081.
21. **Ren, B., H. Cam, Y. Takahashi, T. Volkert, J. Terragni, R. A. Young, and B. D. Dynlacht.** 2002. E2F integrates cell cycle progression with DNA repair, replication, and G(2)/M checkpoints. Genes Dev. **16:**245–256.
22. **Rizos, H., E. Diefenbach, P. Badhwar, S. Woodruff, T. M. Becker, R. J. Rooney, and R. F. Kefford.** 2003. Association of p14ARF with the p120E4F transcriptional repressor enhances cell cycle inhibition. J. Biol. Chem. **278:**4981–4989.
23. **Rooney, R. J.** 2001. Cell cycle attenuation by p120E4F is accompanied by increased mitotic dysfunction. Cell Growth Differ. **12:**505–516.
24. **Rooney, R. J., R. R. Daniels, N. A. Jenkins, D. J. Gilbert, K. Rothammer, S. W. Morris, D. R. Higgs, and N. G. Copeland.** 1998. Chromosomal location

and tissue expression of the gene encoding the adenovirus E1A-regulated transcription factor E4F in humans and mice. Mamm. Genome **9:**320–323.
25. **Rooney, R. J., K. Rothammer, and E. R. Fernandes.** 1998. Mutational analysis of p50E4F suggests that DNA binding activity is mediated through an alternative structure in a zinc finger domain that is regulated by phosphorylation. Nucleic Acids Res. **26:**1681–1688.
26. **Saccone, S., P. Sandy, G. Meroni, M. Gostissa, G. Della Valle, and G. Del Sal.** 1998. Assignment of the E1A-regulated transcription factor E4F gene (E4F1) to human chromosome band 16p13.3 by in situ hybridization and somatic cell hybrids. Cytogenet. Cell Genet. **82:**99–100.
27. **Sandy, P., M. Gostissa, V. Fogal, L. D. Cecco, K. Szalay, R. J. Rooney, C. Schneider, and G. Del Sal.** 2000. p53 is involved in the p120E4F-mediated growth arrest. Oncogene **19:**188–199.
28. **Schmidt-Kastner, P. K., K. Jardine, M. Cormier, and M. W. McBurney.** 1998. Absence of p53-dependent cell cycle regulation in pluripotent mouse cell lines. Oncogene **16:**3003–3011.
29. **Song, M. S., S. J. Song, N. G. Ayad, J. S. Chang, J. H. Lee, H. K. Hong, H. Lee, N. Choi, J. Kim, H. Kim, J. W. Kim, E. J. Choi, M. W. Kirschner, and D. S. Lim.** 2004. The tumour suppressor RASSF1A regulates mitosis by inhibiting the APC-Cdc20 complex. Nat. Cell Biol. **6:**129–137.
30. **Stevaux, O., and N. J. Dyson.** 2002. A revised picture of the E2F transcriptional network and RB function. Curr. Opin. Cell Biol. **14:**684–691.
31. **Takai, H., K. Tominaga, N. Motoyama, Y. A. Minamishima, H. Nagahama, T. Tsukiyama, K. Ikeda, K. Nakayama, and M. Nakanishi.** 2000. Aberrant cell cycle checkpoint function and early embryonic death in Chk1(−/−) mice. Genes Dev. **14:**1439–1447.
32. **Taylor, S. S., E. Ha, and F. McKeon.** 1998. The human homologue of Bub3 is required for kinetochore localization of Bub1 and a Mad3/Bub1-related protein kinase. J. Cell Biol. **142:**1–11.
33. **Taylor, S. S., and F. McKeon.** 1997. Kinetochore localization of murine Bub1 is required for normal mitotic timing and checkpoint response to spindle damage. Cell **89:**727–735.
34. **Uren, A. G., L. Wong, M. Pakusch, K. J. Fowler, F. J. Burrows, D. L. Vaux, and K. H. Choo.** 2000. Survivin and the inner centromere protein INCENP show similar cell-cycle localization and gene knockout phenotype. Curr. Biol. **10:**1319–1328.
35. **Wells, J., C. R. Graveel, S. M. Bartley, S. J. Madore, and P. J. Farnham.** 2002. The identification of E2F1-specific target genes. Proc. Natl. Acad. Sci. USA **99:**3890–3895.
36. **Winston, N., F. Bourgain-Guglielmetti, M. A. Ciemerych, J. Z. Kubiak, C. Senamaud-Beaufort, M. Carrington, C. Brechot, and J. Sobczak-Thepot.** 2000. Early development of mouse embryos null mutant for the cyclin A2 gene occurs in the absence of maternally derived cyclin A2 gene products. Dev. Biol. **223:**139–153.